## 6. RESEARCH PROGRAM, ACCOMPLISHMENTS, AND PLANS

**Period:** March 15, 2006 to March 15, 2007

## RESEARCH PROGRAM

**Overview:**

Our Nanoscale Science and Engineering Center develops tools to study nanoscale systems. We would like to develop future electronic and photonic devices that control electrons and photons in nanostructures. The Center plans to do this by synthesizing nanoscale building blocks and developing new imaging techniques. We would also like to better understand how biological systems function at the nanoscale by developing tools based on the Physical Sciences.

Three Research Clusters address these goals:

**Cluster I: Tools for Integrated Nanobiology** builds bridges between the Physical Sciences, Biology, and Medicine. The Physical Sciences offer powerful new tools for manipulating and testing biological cells and tissues, based on microfluidic systems, soft lithography, and semiconductor technology. In turn, Biology and Medicine offer an enormous range of engaging problems in functional biological systems, and the opportunity to think about "hybrid" systems that combine biological and non-biological components.

**Cluster II: Nanoscale Building Blocks** addresses the synthesis of new classes of nanostructures that exhibit size-dependent properties. An emphasis is placed on zero, one and two-dimensional nanostructures, including the development of nanoparticle and nanowire heterostructures. Techniques to synthesize nanostructures from new materials are being developed, including oxide semiconductors and metal chalcogenides. These nanoscale building blocks provide new approaches for nanoelectronics and nanophotonics as well as sensors for biological systems.

**Cluster III: Imaging at the Nanoscale** explores new ways to image the quantum behavior of electrons and photons in nanostructures using custom-made scanning probe microscopes (SPMs). New instruments include a liquid-He cooled Scanning Tunneling Microscope (STM) and a Nearfield Scanning Optical Microscope with custom tips. These add to previously developed instruments for Ballistic Electron Emission Microscopy (BEEM), a dual tipped STM, and cooled SPMs for capacitive probing of electrons. These tools are used to develop devices for nanoelectronics and nanophotonics, and qubits for quantum information processing. Semiconductor heterostructures with novel properties are grown for this work using Molecular Beam Epitaxy at UC Santa Barbara.

**CLUSTER 1: Tools for Integrated Nanobiology**

*Coordinator*: **George M. Whitesides**

Donhee Ham (SEAS, Harvard)  Howard A. Stone (SEAS, Harvard)
Efthimios Kaxiras (Physics & SEAS, Harvard)  Robert M. Westervelt (SEAS & Physics, Harvard)
Joseph Mizgerd (SPH, Harvard)  George M. Whitesides (Chemistry, Harvard)
Kevin (Kit) Parker (SEAS, Harvard)  Xiaowei Zhuang (Chemistry, Physics, Harvard)

*Collaborators*: Rick Rogers (School of Public Health, Harvard) Giannoula Klement (Children's Hospital, Harvard), Ralph Weissleder (Medical School, Harvard), Mara Prentiss (Physics, Harvard), and X. Sunney Xie (Chemistry, Harvard)

*Number of postdoctoral fellows:* 3
*Number of graduate students:* 5
*Number of undergraduate students:* 4

**Introduction**

As biology begins to ask more quantitative and analytical questions about the nature of the cell, it needs new tools to study subcellular structures that have nanoscale dimensions. An important task is to build bridges between the physical and biological sciences. The physical sciences offer to biology new measurement tools and new procedures for analyzing the information obtained. In turn, biology offers to the physical sciences an enormous range of engaging problems, and stimulating examples of very sophisticated, functional biological systems. It also offers the opportunity to think about "hybrid" systems that combine biological and non-biological components.

The interface between the biological and physical sciences is one with enormous promise for fundamentally new science and, ultimately, technology. By supporting collaborations between investigators in the School of Engineering and Applied Sciences (SEAS), the Dept. of Chemistry and Chemical Biology, the Medical School, and the School of Public Health at Harvard, Cluster I will catalyze and expand a series of very effective collaborations across the physical-biological interface.

We expect three outcomes:

*Tools for Cellular Biology and Tissue Culture:* One of the major contributions that the physical sciences can offer to biology are new physical tools that can provide new kinds of information about cells and tissues.

*The Science and Engineering of Interfaces between Animate and Inanimate Systems:* This research will contribute to studies of cells in cell cultures, and to the assembly of groups of cells of the same or different types. In society, it will contribute to engineering the interface between patients and prostheses.

*Tools for the Development of Drugs:* The control over cells afforded by new microfluidic tools will be the basis for entirely new types of bioassay that will be important as the pharmaceutical industry moves away from information-poor animal

assays in preclinical studies toward more informative studies based on primary human cells.

**Major Accomplishments**

Research in *Tools for Integrated Nanobiology* cluster is advancing our ability to manipulate individual biological cells, and to study their interior using new probes.

**Kit Parker** is developing an atomic force microscope (AFM) with specially coated conducting tips that can selectively bond to particular proteins. By changing the sign of the tip voltage, the bonding can be turned on or off. By combining imaging with manipulation, this AFM can conduct image-guided cell surgery with molecular sensitivity. One can target, manipulate and extract items of interest. **Parker** has demonstrated this approach by using an AFM tip coated with polypyrrole, doped with anti-fibronectin, to pick up and move a fluorescent bead coated with fibronectin (FN).

**Xiaowei Zhuang** is investigating ways to image biomolecules and their interactions *in vivo* with high spatial and temporal resolution. Raman scattering has the potential for chemical imaging, but the cross section is far less than fluorescence from dye molecules at the single molecule level. **Zhuang** aims to make nanoparticles that not only have a bright fluorescence, but also greatly enhance the Raman scattering of nearby molecules. She has synthesized a new class of silver nanostructures which exhibit extremely strong fluorescence and enormous Raman enhancement with factors on the order of $10^{14}$–$10^{15}$. In the next two years, she plans to use these superclusters for tracking individual protein and RNA molecules in live cells.

**Donhee Ham** and **Robert Westervelt** have developed hybrid CMOS/Microfluidic chips for the manipulation of biological systems that combine the power of integrated circuit technology with the biocompatibility of microfludics. A custom integrated circuit (IC) is made at a foundry, and the microfluidic system is built on top at Harvard. The first ICs contained a two-dimensional array of microcoils that acted like a display – when energized they could trap and move a magnetic-bead tagged cell through the microfluidic system above. **Ham** is now developing ICs to sense the prescence of a magnetic bead in the microlfuidic chamber using RF magnetic fields. This research is aimed at developing chips that show the location of a tagged cell, in addition to trapping and moving it. Lee, **Ham** and **Westervelt** edited a book titled *CMOS Biotechnology* for Springer with chapters describing ways to use semiconductor technology to develop tools for biology and medicine.

**Nano- and Microscale Tools for Use in Molecular and Cell Biology**

**George M. Whitesides**
Chemistry, Harvard University
*Collaborators*: Federico Capasso (Harvard)

***Organic Metal-Insulator-Metal (MIM) Junctions***. We are investigating electron transport across metal-insulator-metal junctions, in which the "insulator" is a self-assembled monolayer (SAM, or two face-to-face SAMs). We are developing these systems as models with which to study charge transport in nm-scale organic thin films; this work is an integral part of the growing area of organic electronics. We have made a number of important technical advances this year:

i) The system on which we have spent most of our efforts has been one in which one electrode is a gold or silver thin film which supports a SAM. The second electrode is a conformal drop of mercury, supporting a second SAM. This second SAM is necessary to avoid failure of the junction. We have found that by working with so-called "template stripped" metal we can dramatically improve the performance of this electrode. In template stripping, we evaporate the gold or silver on a flat substrate (typically $Si/SiO_2$) wafer, support this film with a macroscopically thick layer of adhesive (connected to a glass slide) or solder, and then crack the system from the $Si/SiO_2$ layer (to which it adheres poorly). The resulting surfaces are substantially flatter than those prepared by evaporation direction, and when SAMs are prepared on them, they yield MIM junctions that give much more reproducible results than those obtained using evaporated surfaces.
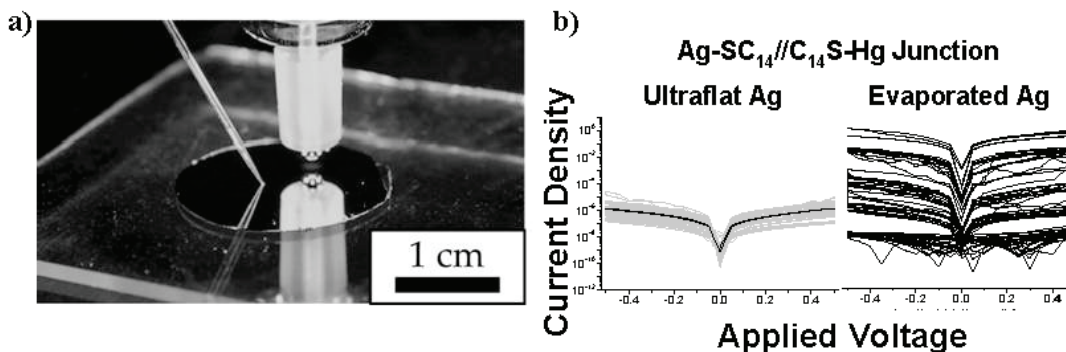


**Figure 6.1.1 a)** Photograph of a template-stripped Ag surface on a glass mechanical support, and contacted with a gold needle. Above the surface hovers a drop of mercury suspended from a syringe. **b)** Plots of the average current density-voltage curves (bold black lines) and all current density-voltage curves (light gray lines) measured on the bilayer junctions using SAMs of alkanethiolate ($SC_{14}$) on ultraflat silver (*left*) and using SAMs of $SC_{14}$ on evaported silver (*right*). Upon switching to the ultraflat silver, the range in measured values of current density decreased by more than $10^6$.

ii) We have developed a system in which the top metal contact is a layer of a low-melting In/Ga eutectic. This system further improves reproducibility, by decreasing the sorting that comes (we believe) from formation of filaments between the mercury drops used previously and the gold or silver substrate.
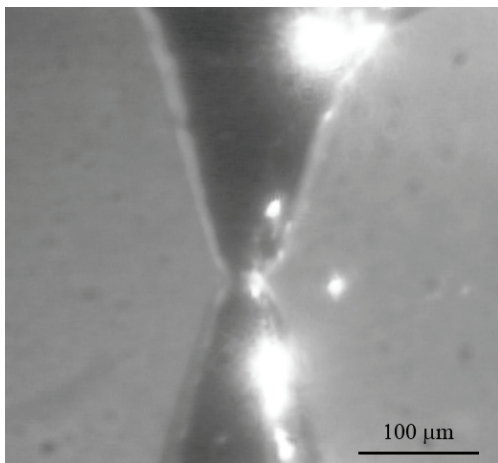
**Figure 6.1.2.** An SAM of $SC_{14}$ on Ag, contacted with an In/Ga electrode. We perform measurements on this type of junction reproducibly in air.

iii) We have developed a new kind of system in which the two SAMs (in this instance comprising $-CO_2^-$ head groups) sandwich a thin layer of electrolyte containing a redox active cation (Ru(II/III) in most of our work). This system is a very effective one for exploring nanoscale electrochemistry.

The combination of these technical advances is a *much* improved reliability in these systems, and data that are much more tightly clustered around a central value. We are now finally approaching our long-term objective of a test system that will enable us to explore the physical-organic chemistry of charge transport (almost certainly by tunneling, and in most cases by hole tunneling rather than electron tunneling). We propose to expand the range of substrates that we explore beyond simple n-alkanethiolates in the future, and to continue to work on defining the system in terms of statistics.

*Nanoskiving*.  We have developed an extraordinarily useful system in which we make nanostructures by a process that involves depositing thin (10–20 nm) metal films on a topographically contoured surface of an appropriate epoxy resin, embedding this structure in further epoxy, and finally sectioning it with an ultra microtome. This procedure makes metallic nanostructures in which the dimensions of the wires (10–20 nm for the deposited metal film, 0.5–2.0 µm for the topographically structured features, and, amazingly, 20 nm for the thickness of the section cut by the microtome. These nanostructures, which can be made in large arrays, are among the most regular that have been made, and are certainly a facile route to simple nanostructures.

We, with **Federico Capasso** in the SEAS, have begun to apply these structures in optics. We have explored simple wires as plasmonics structures, and more complex structures ("L" shapes, and squares with rounded corners) for bandstop filters in the mid-infrared (5–15 µm) region. The performance of the system is excellent, and these systems provide what is probably the only *practical* route into these kinds of structures. Having established that this fabrication method works very well, we intend in the next year to develop it as an entry into a range of nanostructures.

*Bubbles as Complex Systems*.  We are continuing an extended project—carried out primarily with DoE support but requiring extensive use of NSEC facilities, and collaboration with NSEC staff) that looks at bubbles of gas moving through microfluidic channels. These systems have astonishingly complex and useful behaviors, which are often determined by the characteristics of thin films of fluid that range from a few microns to a few hundred nanometers thick (between the bubble and the walls of the channel). We are applying these systems of bubbles in microchannels for a range of

applications: making monodisperse microstructures, coding information, mixing fluids in low Reynolds number flows, "solving" mazes, and others.
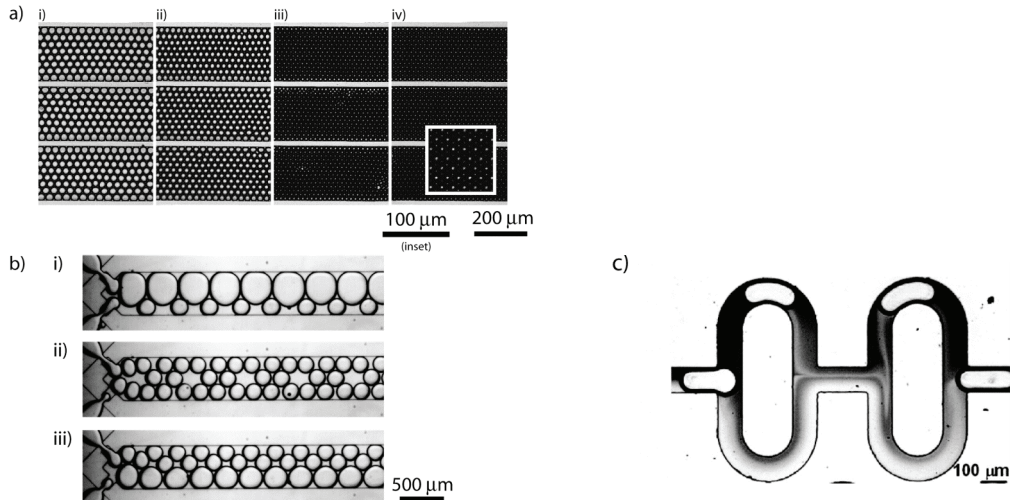


**Figure 6.1.3. a)** Two-dimensional, hexagonal flowing lattice of bubbles. Flow parameters (i.e., rate of the flow of continuous fluid, and pressure of gas) control the diameter of the bubbles—periodicity of the lattice structure. **b)** Flowing lattice of droplets. We used two flow-focusing generators of droplets to form stable lattice structure. Each generator of droplets is individually addressable, allowing to achieve binary lattice structures. **c)** Mixing of co-laminar flow at low Reynolds number. Introduction of flowing bubbles to co-laminar flow enhances the mixing of two streams that is otherwise mixed only under diffusion.

# Microscale Instrumentation to Dynamically Control Protein-Protein Interactions

**Kevin Kit Parker**
Bioengineering Harvard
*Collaborators*: Robert M. Westervelt

Micro- and nanotechnologies are emerging as promising platforms for biomedical analysis, since they often yield new insights into gene and protein ensembles that trigger pathological abnormalities. Existing micro- and nanoscale devices can map genome sequences of interest [Park and Swerdlow, 2003; Auroux *et al.*, 2004; Chou *et al.*, 1999], quantify protein expression levels [Hutterer and Dolnik, 2003; Maerkl and Quake, 2005; Yang *et al.*, 2003], detect the onset of cancer [Seligson, 2005], and measure variations in gene expression in small populations of cells [Chou *et al.*, 1999; Liu *et al.*, 2005]. Moreover, these biotechnologies can be used to measure molecular concentration gradients in a rapid and high throughput fashion via surface modifications of individual micro- and nanoscale components
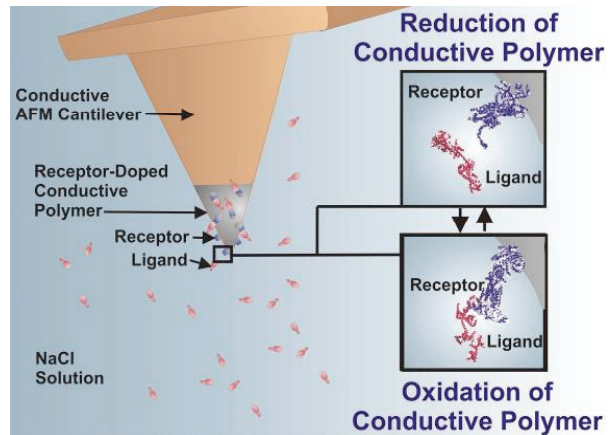


**Figure 6.1.4**. Microfabricated cantilevers functionalized with receptor-doped conductive polymers can be used to dynamically modulate protein-protein interactions at the micro- and nanoscale by controlling the oxidation and reduction states of the polymer.
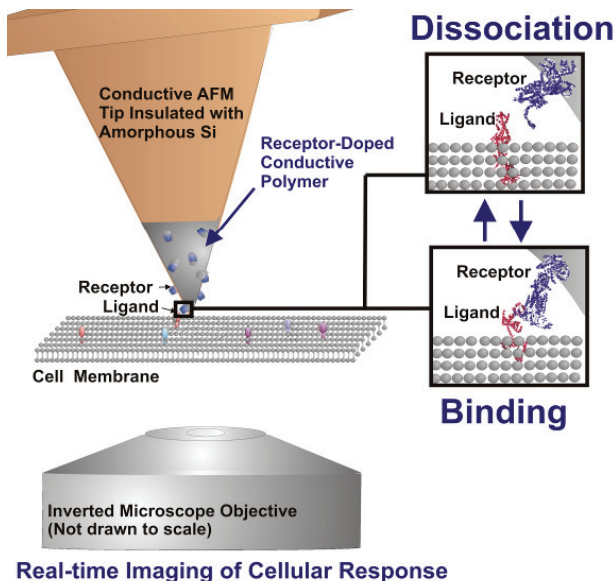


**Figure 6.1.5.** Conductive polymer/AFM devices can be utilized to examine cell and tissue physiological responses under biochemical and/or mechanical stimulation.

[Maerkl and Quake, 2005; Quake, 2004; Basttiston *et al.*, 2001]. However, existing micro- and nanoscale devices are unable to probe cell function at the length scale of protein complexes [Helmke and Minerick, 2006]. Yet, the ability to actively control protein-protein interactions at the micro- and nanoscale could be exploited to detect and repair cellular dysfunction, quantify biological toxins, or investigate the effectiveness of pharmaceutical leads. In addition, the capability to mediate cell function via specific protein complexes would permit investigators to elucidate the dynamic nature of signaling cascades involved in cancer and heart disease progression.
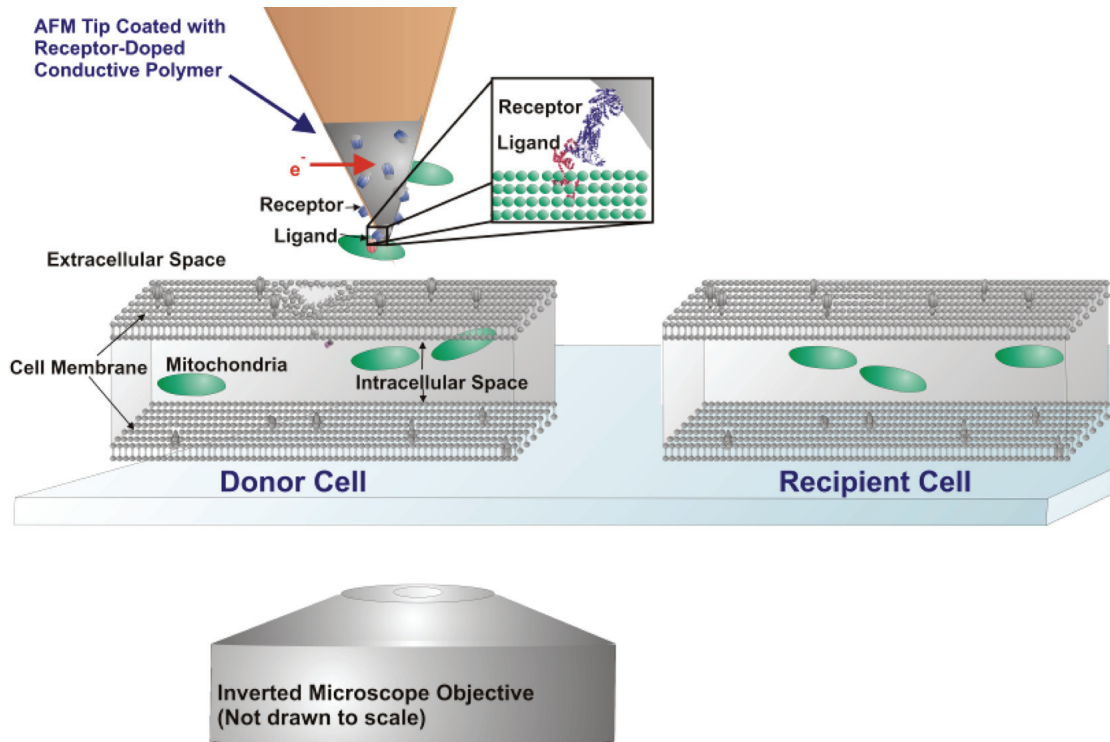
**Real-time Imaging of Mitochondrial Transport**

**Figure 6.1.6**. Assembly of a 'metabolic super cell' using microsurgical instrumentation with molecular specificity. Mitochondria are extracted from a donor cell using the receptor-doped conductive polymer/AFM technology, where the receptors embedded in the conductive polymer are specific for mitochondrial outer membrane proteins. After removal from the donor cell, the mitochondria are subsequently transported to a nearby recipient cell and surgically placed in the cell. Finally, ligand-receptor interactions are inhibited at the AFM tip, thus releasing the mitochondria in the recipient cell.

Towards this end, the research focuses on the development of integrated microelectromechanical systems (MEMS) and conductive polymer instrumentation to selectively and reversibly control protein-protein interactions at the micro- and nanoscale. Specifically, the research involves the development of atomic force microscope (AFM) tips instrumented with a conductive polymer (polypyrrole) to modulate protein-protein interactions (Figure 6.1.4). By combining AFM capabilities with optical and fluorescence imaging modalities, these novel devices will allow investigators to examine cell signaling mechanisms with unprecedented spatiotemporal, mechanical and biochemical control (Figure 6.1.5). Furthermore, the devices can be used to perform image-guided cell nanosurgery with to target, manipulate and extract intracellular structures of interest (Figure 6.1.6).

Overall, the specific aims of my dissertation research are as follows:

1) Selectively and reversibly control protein-protein interactions in an 'on-off' fashion at the *macroscale* (millimeter length scale).

2)  Develop microelectronic devices to mediate protein-protein interactions at the *micro-* and *nanoscale,* as shown in Figures 6.1.4 and 6.1.5.

3)  Use microscale devices to perform image-guided surgical procedures on live cells (Figure 6.1.6).
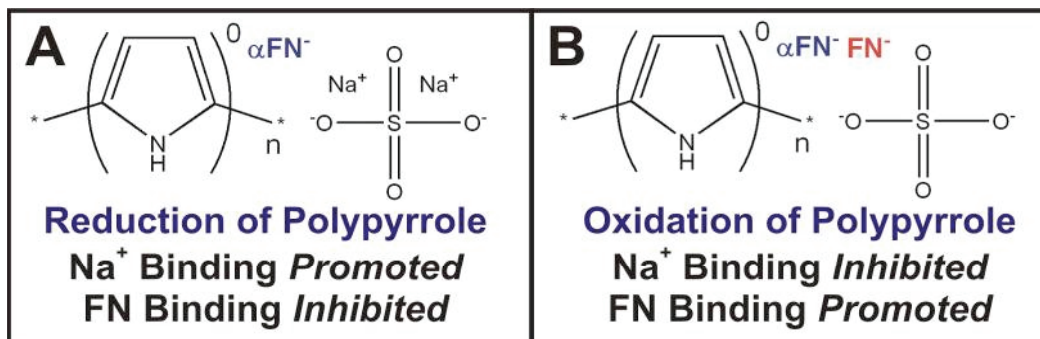


**A**

αFN⁻

**Reduction of Polypyrrole**
Na⁺ Binding *Promoted*
FN Binding *Inhibited*

**B**

αFN⁻ FN⁻

**Oxidation of Polypyrrole**
Na⁺ Binding *Inhibited*
FN Binding *Promoted*

**Figure 6.1.7.** Oxidation and reduction of polypyrrole doped with αFN and sulphate polyions in a physiological salt buffer. During reduction (**A**) of polypyrrole (application of a negative voltage), negative charges in the polymer are neutralized via interactions with Na⁺ ions. Conversely, during oxidation (**B**) of polypyrrole (application of a positive voltage), binding of FN proteins is facilitated such that the polymer matrix remains charge neutral [Gooding *et al*., 2004].

Using macroscale, conductive polymer (polypyrrole) electrodes doped with monoclonal anti-human fibronectin antibodies (αFN), we have verified the ability of these electrodes to bind human fibronectin (FN), a cell adhesion protein, with molecular specificity. Furthermore, we have characterized the ability of αFN-doped polypyrrole electrodes to toggle FN binding in a reversible 'on-off' fashion. A schematic of these chemical interactions is shown in Figure 6.1.7. Application of a negative potential reduces the poly-pyrrole and inhibits FN-αFN interactions (Figure 6.1.7A). Conversely, application of a positive potential oxidizes the polypyrrole and facilitates FN binding to
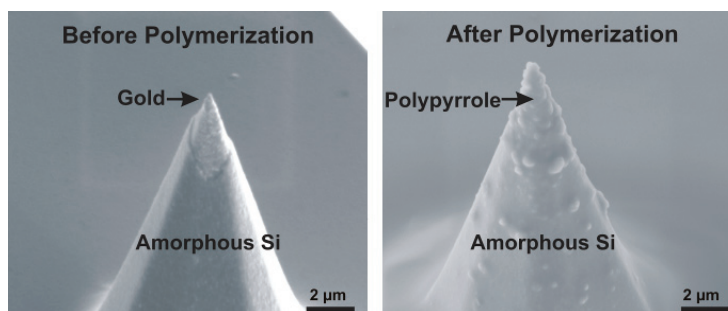


**Figure 6.1.8.** Conductive AFM cantilever tips functionalized with polypyrrole. Gold regions were exposed at the AFM tip (*left*) using a focused ion beam. Polypyrrole was electropolymerized at the AFM tip where the gold is exposed (*right*). Scale bar = 2 microns.

αFN antibodies entrapped in the polypyrrole matrix (Figure 1.7B). In effect, by switching the polymer between the reduction and oxidation states we can control the FN-αFN binding affinity. Although we have been primarily interested in characterizing FN-αFN interactions as a model system, antibody-doped polypyrrole electrodes can be created to selectively and reversibly mediate protein-protein interactions with a myriad of proteins of interest [Gooding *et al*., 2004; Sargent and Sadik, 1999] via the same redox reactions illustrated in Figure 6.1.7.

Results from experiments thus far have shown that:

1)  the extent of FN binding and dissociation can be controlled by the changing the voltage applied to the polypyrrole,
2)  the αFN-doped polypyrrole is specific for FN only (non-specific binding is not an issue),
3)  FN binding to αFN-doped polypyrrole is reversible and highly repeatable.

Exploiting these results, we have fabricated conductive cantilevers with polypyrrole at the AFM tip (Figure 6.1.8). As shown in Figure 6.1.9, integrated αFN-doped polypyrrole/AFM devices can be utilized to transport FN-coated beads (4 μm diameter), demonstrating the ability of these devices to manipulate microscale structures with nanoscale positional control. We have shown that αFN-doped polypyrrole/AFM devices can be used to locate, move and release FN-coated fluorescent beads, which illustrates the potential of this conductive polymer/AFM technology to modulate protein-protein interactions with incredible spatial and molecular control. We have also established that these polypyrrole/AFM devices bind and release FN proteins with molecular specificity at the micro- and nanoscale. In effect, our results d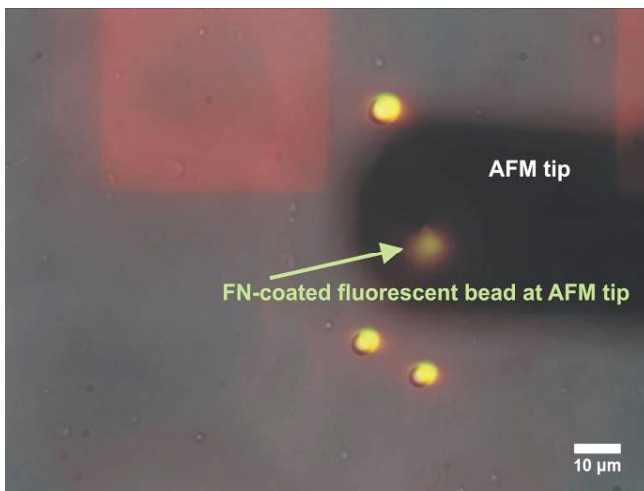emonstrate that the capability to control protein-protein interactions can be exploited at the micro- and nanoscale, which may ease the incorporation of this novel polymer into innovative biomedical technologies. We hold a provisional patent on this technology and we are currently submitting these results for publication.



**Figure 6.1.9.** Movement of a FN-coated fluorescent bead using a αFN-doped polypyrrole AFM tip. AFM binding to a FN-coated bead (green circles, 4 μm diameter) was facilitated by placing the tip at the bead surface. The bead was lifted and moved 65 μm across the coverslip. The red squares are rhodamine-labeled, micropatterned FN to serve as fiducial markers of bead location.

Spatiotemporal, mechanical and biochemical control of protein-protein interactions will allow us to further elucidate subcellular signaling mechanisms which underlie the progression of heart disease. Specifically, future research will focus on the use of these innovative AFM devices to examine the relationship between mechanosensitive ion channels, cytoskeletal architecture and calcium dynamics, all of which have been shown to be important mediators of heart disease [Sadoshima *et al*., 1992; Gomez *et al*., 2001; von Lewinski *et al*., 2004]. The devices will also be used to investigate the effects of cytoskeletal architecture and force transmission on nuclear morphology in healthy and diseased cardiac cells. Distorted nuclear morphologies have been shown to significantly alter gene expression profiles [Thomas *et al*., 2002], which may exacerbate heart disease progression.

Moreover, the polypyrrole/AFM devices will be used to perform image-guided surgical procedures on live cells (Figure 6.1.6). Since surgical precision is often limited by the manual dexterity of the surgeon, damage to small capillaries and vessels during surgery can easily occur, which may aggravate existing pathologies. Therefore, by using the polypyrrole/AFM devices to complete micro- and nanoscale surgical procedures (Figure 6.1.6), we will establish that the technology can be utilized to target and surgically extract specific cell types and intracellular structures of interest.

## References:

Auroux, P.A., Koc, Y., deMello, A., Manz, A., and Day, P.J.R., "Miniaturised nucleic acid analysis," *Lab on a Chip* **4**, 534–546 (2004).

Battiston, F.M., J.-P. Ramseyer, H.P. Lang *et al.,* "A chemical sensor based on a microfabricated cantilever array with simultaneous resonance-frequency and bending readout," *Sensors and Actuators B-Chem.* **77**, 122–131 (2001).

Chou, H.P., Spence, C., Scherer, A., and Quake, S., "A microfabricated device for sizing and sorting DNA molecules," *Proc. Natl Acad. Sci., USA* **96**, 11–13 (1999).

Gomez, A.M., Guatimosim, S., Dilly, K.W., Vassort, G., and Lederer, W.J., "Heart failure after myocardial infarction—Altered excitation-contraction coupling," *Circ.* **104**, 688–693 (2001).

Gooding, J.J., C. Wasiowych, D. Barnett *et al.,* "Electrochemical modulation of antigen-antibody binding," *Biosensors & Bioelectronics* **20**, 260–268 (2004).

Helmke, B.P. and Minerick, A.R., "Designing a nano-interface in a microfluidic chip to probe living cells: Challenges and perspectives," *Proc. Natl Acad. Sci. USA* **103**, 6419–6424 (2006).

Hutterer, K. and Dolnik, V., "Capillary electrophoresis of proteins 2001–2003, *Electrophoresis* **24**, 3998–4012 (2003).

Liu, J., Quake, S., Williams, B.A., Gwirtz, R.M., and Wold, B.J., "Microfluidic microarrays for gene expression studies," *Biophys. J.* **88**, 543A (2005).

Maerkl, S. and Quake, S., "High-throughput synthesis and functional screening of proteins using MLSI," *Biophys. J.* **88**, 658A (2005).

Park, S.R. and Swerdlow, H., "Concentration of DNA in a flowing stream for high-sensitivity capillary electrophoresis," *Analyt. Chem.* **75**, 4467–4474 (2003).

Quake, S., "Biological large-scale integration," *Abstracts of Papers of the Am. Chem. Soc.* **227**, U116 (2004).

Sargent, A. and Sadik, O.A., "Monitoring antibody-antigen reactions at conducting polymer-based immunosensors using impedance spectroscopy," *Electrochimica Acta* **44**, 4667–4675 (1999).

Sadoshima, J., Takahashi, T., Jahn, L., and Izumo, S., "Roles of Mechanosensitive Ion Channels, Cytoskeleton, and Contractile Activity in Stretch-Induced Immediate-Early Gene-Expression and Hypertrophy of Cardiac Myocytes," *Proc. Natl Acad. Sci., USA* **89**, 9905–9909 (1992).

Seligson, D.B., The tissue micro-array as a translational research tool for biomarker profiling and validation, *Biomarkers* **10**, S77–S82 (2005).

Thomas, C.H., Collier, J.H., Sfeir, C.S., and Healy, K.E., "Engineering gene expression and protein synthesis by modulation of nuclear shape," *Proc. Natl Acad. Sci., USA* **99**, 1972–1977 (2002).

von Lewinski, D., Stumme, B., Fialka, F., Luers, C., and Pieske, B., "Functional relevance of the stretch-dependent slow force response in failing human myocardium" *Circ. Res.* **94**, 1392–1398 (2004).

Yang, X.H., Zhang, X.M., Li, A.Z., Zhu, S.Y., and Huang, Y.P., "Comprehensive two-dimensional separations based on capillary high-performance liquid chromatography and microchip electrophoresis," *Electrophoresis* **24**, 1451–1457 (2003).

**Development and Characterization of a Cellular-Scale Differential Manometer Modelling of an Artificial Flagella**

**Howard A. Stone**
Materials and Fluid Mechanics, Harvard University
*Collaborators*:  J. Bibette (ESPCI, Paris), George M. Whitesides (Harvard)

My research group has pursued three distinct areas of research for the NSEC: (i) *Development and characterization of a cellular-scale differential manometer* (reported in *PNAS* 2006) and (ii) *Modelling of an artificial flagella* (reported in *Nature* 2005 and the *Journal of Fluid Mechanics* 2006). In addition, during the past year we have been imaging and studying remarkably order nanoscale patterns that form on the surface of micron-diameter bubbles in foams. All three projects are being continued. The projects are part of the NSEC effort in *Tools for Integrated Nanobiology*. The projects have engaged undergraduates. Also, the research has included experimental contributions and theoretical and numerical advances.

In the first project we have designed a new approach to probe the mechanical response of cells under continuous flow conditions. Since most if not all existing mechanical measurements on individual cells examine cells that are stationary on substrates, the opportunity to investigate, even qualitatively, the mechanical response for cells flowing continuously through a device may offer new ideas in cellular-scale sensing. Our most recent studies have been focussed on measuring ATP release as a function of deformation of the cell. We have been doing this with channels small enough that we can make measurements of individual cells. We believe these would be the first direct cellular-scale measurements of deformation-induced ATP release (previous work as been based on statistics for populations of cells).

In the second project we have collaborated on what is likely the first micron-scale flagella-like element, which can swim in controlled directions.

(i)     *Development and characterization of a cellular-scale differential manometer*: It is known that the mechanical properties of cells are linked to some diseases (e.g., malaria). In addition, chemicals are known to affect the mechanical response of cells. We have developed a microfluidic device with dimensions comparable to individual red blood cells, which provides an indication of the change of pressure when the cell enters the smallest channel (see Figure 6.1.10: *left* and *middle*). The methodology in principles works for any kind of small or flexible object and has a time resolution on the order of milliseconds. The measurement can be performed even when cells undergo lysis (see Figure 6.1.10, *right*) and can distinguish cells that have been made more rigid by addition of gluteraldehyde. These results suggest that this continuous flow approach to sensing changes in mechanical properties of cells can be accomplished and combined with the flexibility of microfluidic approaches for controlling chemical composition. We are currently pursuing several new directions of this project.

More recent work has included the development of numerical simulation tools for these kind of flow situations and additional controlled experiments probing the influence of chemicals on the mechanical response of the cells.

(ii)    *Modelling of an artificial flagella*: In a collaboration with the group of J. Bibette (ESPCI, Paris) we studied the first artificial flagella ever created. The Paris group created the object and experimentally demonstrated the idea and we developed a continuum description of the magneto-elastic filament. The micron-length slender elastic object consists of magnetic nanometer-diameter spheres tied together using DNA and biotin-streptavidin links. The slender filament can be aligned along the direction of a constant externally applied magnetic field. Application of a transverse magnetic field causes a wave to travel along the filament and if fore-aft symmetry is broken, the filament swims. Symmetry breaking was shown to happen naturally owing to inevitable defects, or could be produced by tying the filament to a large object. By attaching the filament to a red blood cell, the cell could be transported in a controlled fashion.
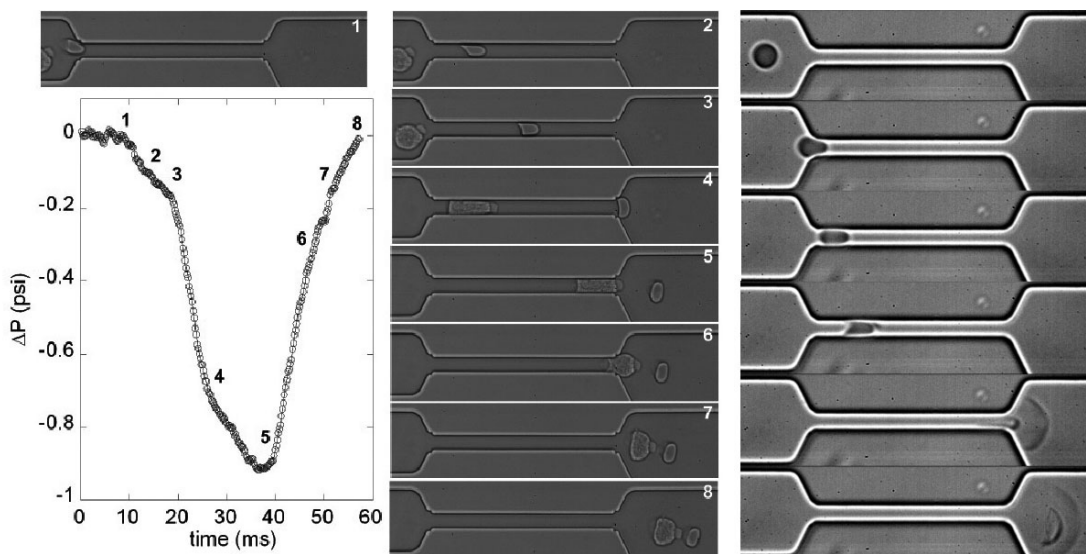


**Figure 6.1.10.** (*Left*, *middle*) Entry of a red blood cell, followed by a white blood cell, into a narrow channel with dimensions comparable to the cell. The pressure change recorded using the manometer we have developed is shown. (*Right*) Flow of a swollen red blood cell into a narrow channel; lysis occurs.

Our most recent work has been examining synchronization of driven filaments. The issue of synchronization is key to many natural systems that use filamentary structures. We have constructed a model that now requires numerical simulations. (Figure 6.1.11)

In a third project, in collaboration with Unilever scientists Rodnee Bee (retired) and Alex Lips, along with Dr. David Bell, we have been studying remarkable nanoscale patterns that form on the surface of micron-diameter bubbles that form natural in certain foams.

A typical image is shown in Figure 6.1.12. We have studied many aspects of this system. For example, we have shown that the pattern length scale is at most a weak function of the bubble diameter and the processing conditions. Currently modeling efforts are aimed at understanding the patterns from the properties of the surfactants used to make the foam.
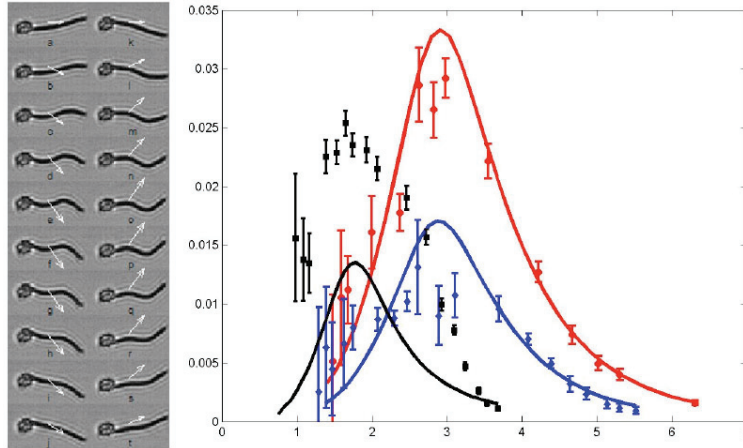


**Figure 6.1.11.** (*Left*) Sequence of deformation of the end of a free filament. The propagation of a bending wave is indicated by the arrows. Conditions for the magnetic field: $B_x$= 9 mT, $B_y$ = 14 mT, f = 20 Hz. Each image corresponds to pictures taken every 2.5 ms. Length of the portion of the filament shown: 34 µm. (*Right*) Scaled velocity as a function of $S_p = L/(\kappa/4\pi\eta)^{1/4}$. Experimental data are discrete points while the continuous lines are the predictions obtained with our model. Error bars are calculated by measuring the drift velocity of a filament when the transverse magnetic field $B_y$ = 0 and by estimating the standard deviation of the bending modulus. The cell radius $a_s$ and the distance $a_l$ of the attachment point from the cell center are evaluated from experimental images. Black squares: Bending modulus k= $3.3.10^{-22}$ J.m, L = 13 µm, $B_x$ = 8.7 mT, $B_y$ = 9.3 mT, $a_s$ = 3.2 µm, $a_l$ = 3.2 µm. Blue diamonds: k = $3.3.10^{-22}$ J.m, L = 21 µm, $B_x$ = 8.7 mT, $B_y$ = 9.3 mT, $a_s$ = 2.7 µm, $a_l$ = 0 µm. Red circles: k = $3.3.10^{-22}$ J.m, L = 24 µm, $B_x$ = 8.9 mT, $B_y$ = 10.3 mT, $a_s$ = 3.1 µm, $a_l$ = 3.1 µm.
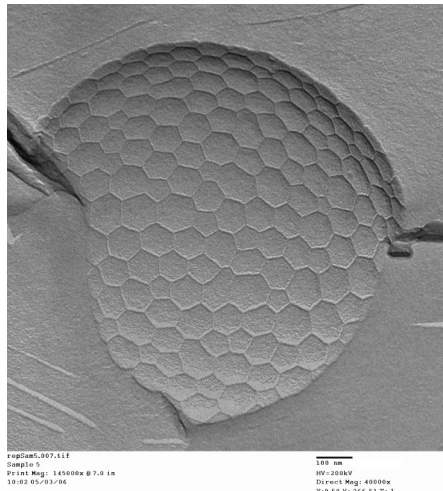


**Figure 6.1.12.** TEM image of nanoscale patterns on the surface of micron-diameter bubbles. The scale bar shown is 100 nm.

52

**Microcoil Array-Based RF Cell Sensors in the CMOS/Microfluidic Hybrid System**

**Donhee Ham**
Electrical Engineering, Harvard University
*Collaborator*: Robert M. Westervelt (Harvard)

**Proposed Goal.** Previously **Robert Westervelt** and I developed a CMOS/ Microfluidic hybrid system for magnetic manipulation of biological cells (Lee *et al.*, 2006, 2007; Lee, **Ham** and **Westervelt**, 2007). Consisting of a CMOS IC and a microfluidic system fabricated on top (Fig. 6.1.13), it can manipulate individual biological cells (tagged by magnetic beads) suspended inside the microfluidic system, by using microscopic magnetic fields produced by a microcoil array (Fig. 6.1.14) in the CMOS chip. Digital electronics controlling the coil array enabled versatile, efficient controls of motions of biological cells.
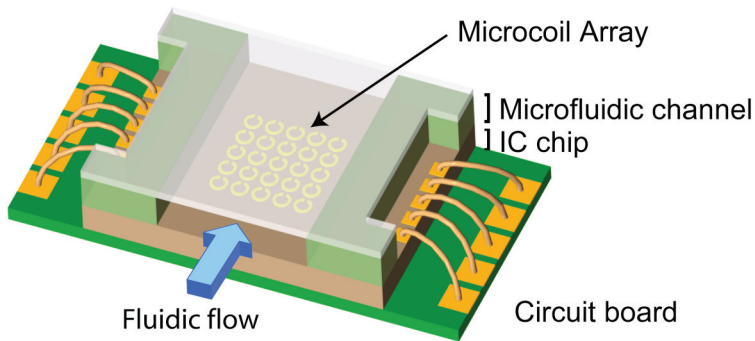


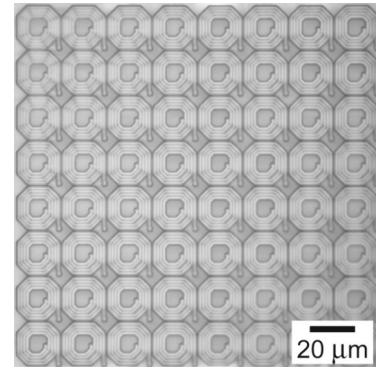**Figure 6.1.13.** Conceptual illustration of a CMOS/Microfluidic hybrid system.



**Figure 6.1.14.** Actual microcoil array in a CMOS IC.

The general goal of our 2006 research was on further developing the hybrid system, by adding a detection capability. We sought to utilize the microcoils used for manipulation for detection as well, by combining them with RF ICs. The basic idea is that a magnetic bead passing over a microcoil will change the coil's reasonance characteristics, which can be detected using RF signals (up to 200 MHz). Since the beads are superparamagnetic, the bead-induced change of the coil character would be small (*e.g.*, inductance change < 1%). Developing a highly sensitive CMOS RF system to sense the small change was at the heart of the effort.

**Approach.** We broke down the development effort for the high-sensitivity CMOS RF system into two parts, (1) development of design techniques for a phase-locked CMOS oscillator to produce a highly-stable, high-purity RF signal on chip, and (2) design of a front-end microcoil-bridge circuit. These represent the two most challenging, yet, requisite tasks to enable the high-sensitivity RF system. Part (1) is important because a stable radio frequency with reduced phase noise is essential in attaining the needed sensitivity to resolve the small, bead-induced change in the coil resonance characteristics. In Part (2), we sought to verify if a magnetic bead indeed induces a change in the coil resonance characteristics by using a stable external Agilent RF signal source. Once this is verified, we could replace the off-chip RF signal source with the on-chip oscillator of Part (1). We

designed circuits for both Parts (1) and (2) in CMOS, which were fabricated in silicon foundry.

**Accomplishments.** For the high-purity CMOS oscillator, we developed an autonomic phase-locked loop (PLL). This PLL constantly measures its undesired input static phase
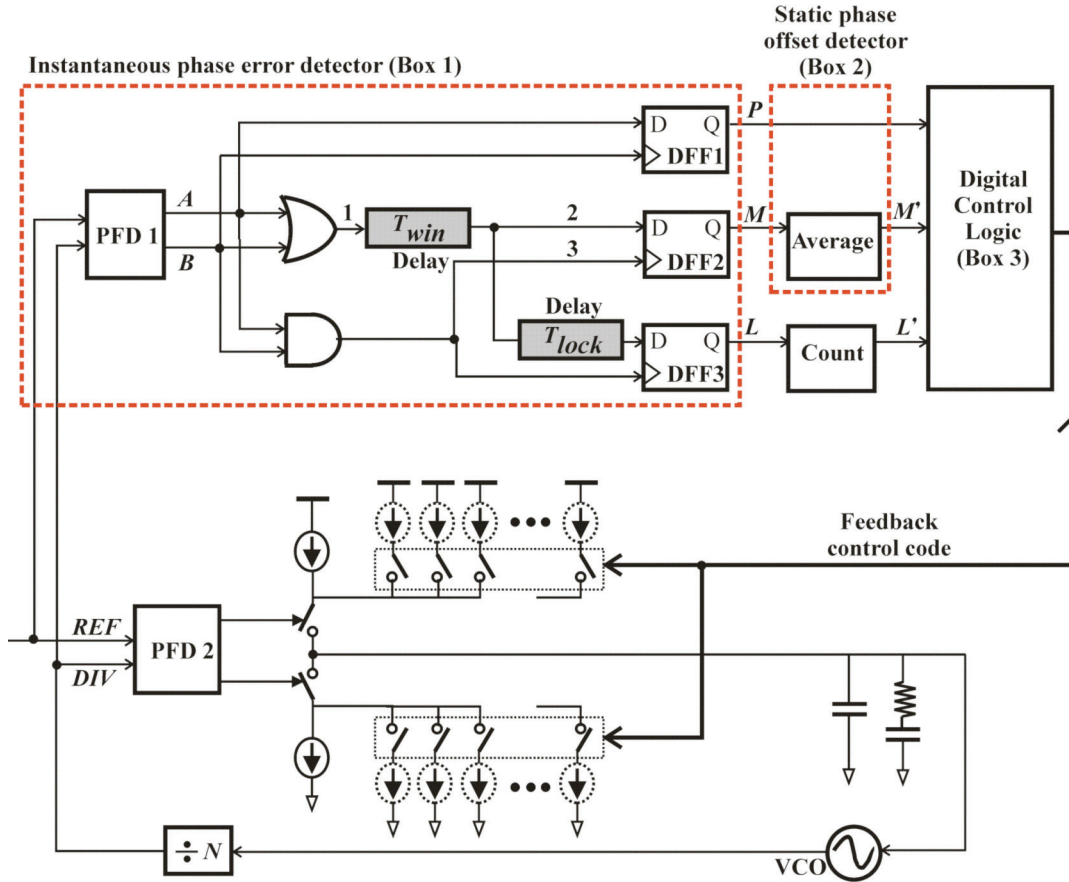


**Figure 6.1.15.** Schematic of the self-adjusting autonomic PLL.

errors, and dynamically self-adjusts for them by reconfiguring loop parameters based upon the measured phase error data. This technique serves to minimize the static phase error that can be always introduced due to process variations. The reduced static phase error corresponds to reduced reference spurs in the frequency domain, corresponding to a high-purity signal. The frequency stability itself is attained by the phase-locking mechanism.

Figure 6.1.15 shows the autonomic PLL's schematic. Charge pump currents are dynamically adjusted by the digital control logic connected to a phase offset detector, which measures static phase offsets to produce feedback signals for the digital control logic. Figure 6.1.16 shows the micrograph of the implemented CMOS IC. Measurements of this circuit showed the reference spur reduction by 5 dB and a static phase offset less

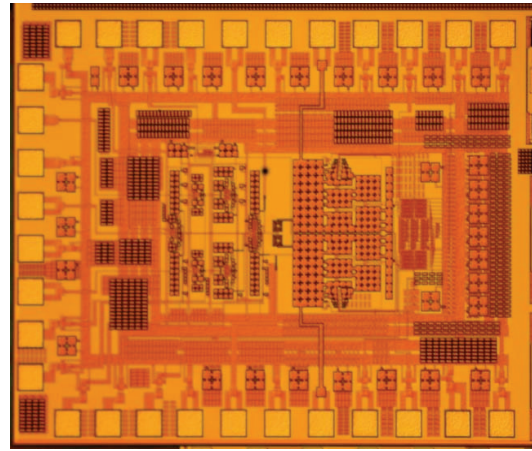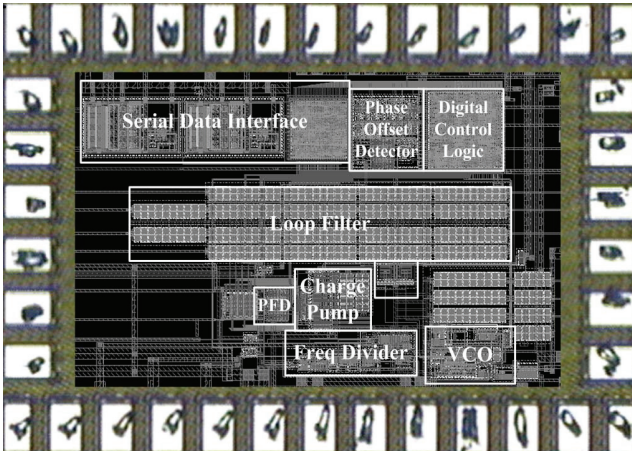than 15 ps, which show the potential of the autonomic PLL for use in the high-sensitivity CMOS RF system.



**Figure 6.1.16.** Die micrograph of the autonomic PLL.



**Figure 6.1.17.** Micrograph of the microcoil

We also implemented the microcoil bridge circuit to experimentally quantify the change in the resonance characteristic of a microcoil induced by a magnetic bead. This chip (Fig. 6.1.17) is currently being characterized using an external RF signal source, which is highly stable.

**Significance.** When the RF system is used with the microcoil array, it would allow imaging of 2-D distribution of bead-bound-cells, where a single microcoil may be thought of as a "pixel". This imaging capability may render bulky optics unnecessary, realizing a true lab-on-a-chip system. Additionally, the RF system may permit sensing of nanomagnetic beads too small to be seen optically. The RF sensor will offer a purely electrical way of sensing cells, not requiring chemical or optical methods.

Hakho Lee, **Donhee Ham** and **Robert M. Westervelt** are Editors of a new book from Springer titled *CMOS Biotechnology* (2007) whose chapters present approaches from Electrical Engineering toward the developement of chips for Biology and Medicine.

**References:**

Lee, Hakho, Yong Liu, Robert M. Westervelt, and Donhee Ham, "IC/Microfluidic Hybrid System for Magnetic Manipulation of Biological Cells," *IEEE Journal of Solid-State Circuits (JSSC)* **41**, 1471 (2006).

Lee, Hakho, Yong Liu, Donhee Ham, and Robert M. Westervelt, "Integrated Cell Manipulation System – CMOS/Microfluidic Hybrid," *Lab. Chip*. **7**, 331 (2007).

Lee, Hakho, Donhee Ham, and R.M. Westervelt, editors, *CMOS Biotechnology,* a book in the series *Integrated Circuits and Systems*, edited by Chandrakasan (Springer, 2007).

# Fluorescent and Raman Active Metal Nanoparticles

**Xiaowei Zhuang**
Chemistry and Physics, Harvard University
*Collaborator*: Charles Lieber (Harvard)

A grand challenge in biological imaging is to develop tools for imaging individual biomolecules and their interactions *in vivo* with high spatial and temporal resolution. While luminescent quantum dots and plasmonic metal nanoparticles overcome the photobleaching of organic dyes and are becoming very promising labels to unravel heterogeneousity in biological processes at the single particle level, none of these labels are able to offer *in situ* chemical information of local environments interacting with the labeled molecules. To overcome this limitation, it is important to create new probes which not only have bright and robust single molecule emission but also are able to report chemical interactions simultaneously. In principle, under light irradiation, even non-fluorescent biomolecules yield Raman scattering, which can provide important environment-dependent spectral signatures of the biomolecules. This Raman scattering process offers a possibility for chemical imaging while tracking *in vivo*. However, the cross section of Raman scattering is generally $10^{15}$ times smaller than fluorescence from dye molecules at the single molecule level. As a part of the Cluster 1-Tools for Integrated Nanobiology, we propose to develop novel probes suitable for long-time tracking and also chemical imaging by creating nanoparticles that not only have bright and robust fluorescence but also greatly enhance the Raman scattering of the nearby molecules.



**Figure 6.1.18.** Fluorescent and Raman active silver nanoparticles. (**A**) Photos of the silver nanoparticle solution with (*left*) and with our (*right*) laser excitation. (**B**) High resolution TEM image of a single silver nanoparticle. (**C**) A live HeLa cell labeled with fluorescent and Raman active silver nanoparticles. (**D**) A surface enhanced Raman spectrum of a single silver nanoparticle on the live HeLa cell surface in 90 pg/ml deurated-glycine solution. Strechtched vibration of C-D of Deurated-glycine was clearly detected by the silver nanoparticle.

Our research goal is developing new metal based probes which can be integrated with single-molecule imaging techniques to offer quantitative chemical information on biological processes at the molecular level. We have synthesized a new class of silver
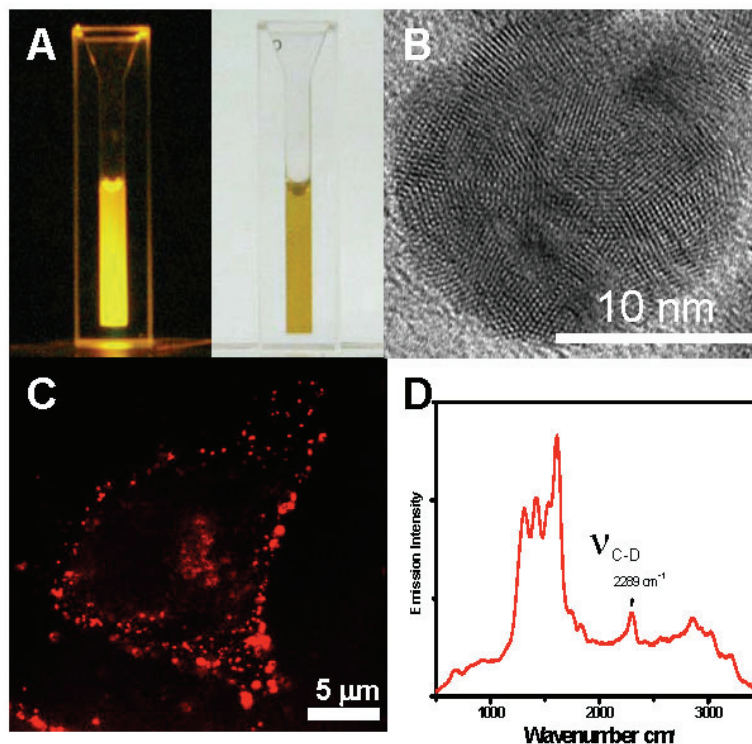
nanostructures which exhibit extremely strong fluorescence with cross section about $10^{-14}/cm^2$ and enormous Raman enhancement with factors on the order of $10^{14}$–$10^{15}$ (Fig. 6.1.18A). Using high resolution transmission electron microscopy and photoelectron spectroscopy in Center of Nanosystems at Harvard, we were able to characterize the detailed polycrystalline structures of these fluorescent and Raman active silver nanoparticles (Fig. 6.1.18B)—each nanoparticle appears to be made of a large number of small single-crystal nanoclusters. A unique electronic structure of these novel fluorescent and Raman active silver nanoparticles is manifested by continuous excitation and discrete emission. The ultrabright emission allows single particles of such nanostructures to be readily visualized in live cells (Fig. 6.1.18C). The giant Raman enhancement effect allows visualizing vibrational information of chemical bonds of a single small molecule in the vicinity of the silver nanoparticle (Fig. 6.1.18D). Robust emission, giant Raman enhancement and high optical purity make these silver nanoparticles promising bioprobes with an extra capability of providing chemical information on the microenvironments inside living cells.

In these next 1–2 years, we plan to accomplish the following aims:

1. Functionalize surface of these superclusters for specific labeling of biomolecules.

2. Use these superclusters as labels for tracking individual protein and RNA molecules in live cells.

3. Investigate the mechanism of Raman-enhancement effect of these silver nanocrystals. We will utilize this large Raman enhancement effect to detect distributions of drug molecules and metabolites in a living cell.


**Snapshot of DNA Translocation Through a Nanopore**

**Efthimios Kaxiras**
Physics and Applied Physics, Harvard University
*Collaborator:* George M. Whitesides (Harvard)


Biological systems exhibit a complexity and diversity far richer than the simple systems traditionally studied in physics or chemistry. The powerful quantitative methods developed in the latter two disciplines to analyze the behavior of prototypical simple systems are often difficult to extend to the domain of biological systems. Interest in studying these systems is steadily growing, which provides strong incentive to develop new methods both experimentally and theoretically. Advances in computer technology and breakthroughs in simulational methods reduce the gap between quantitative models and actual biological behavior. The main challenge remains the wide and disparate range of spatio-temporal scales involved in the dynamical evolution of complex biological systems. In response to this challenge, various strategies have been developed, which are in general

referred to as *multiscale modeling*. Here, we have used two different *multiscale* approaches to simulate biological systems and investigate their physical properties.

## 1. Multiscale Modeling of DNA Translocation through Nanopores

We have recently developed a composite multi-scale framework that involves different levels of the statistical description of matter (continuum and atomistic) and is able to handle different scales. This is feasible through the spatial and temporal coupling of a *mesoscopic* fluid solvent, the lattice Boltzmann method [Wolf-Gladrow, 2000; Succi, 2001], with the atomistic level, which employs explicit molecular dynamics. Within this scheme information is exchanged between the scales. The solvent dynamics is represented through a discrete set of pre-averaged probability distribution functions, which are propagated along straight particle trajectories. This dual field/particle nature greatly facilitates the coupling between the *mesoscopic* fluid and the atomistic levels, which proceeds seamlessly in time and only requires standard interpolation/extrapolation for information-transfer in physical space.
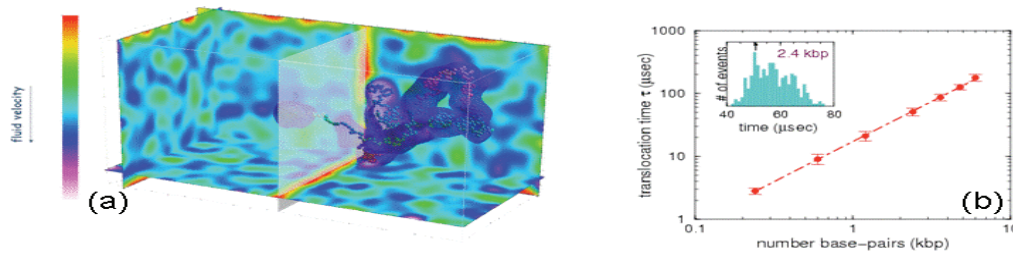


**Figure 6.1.19.** (**a**) 3-D visualization of the translocation process through a nanopore: The molecule as it passes through the pore is shown, together with the fluid velocity mapped by contour plots on different planes and by a 3-D representation in the vicinity of the beads. (**b**) Scaling law of the translocation time with the DNA length. The translocation time for each length is identified by the most probable time at the maximum of all duration histograms, similar to the one in the inset for 2.4 kpb (the arrow shows the most probable time for this length).

Motivated by recent experiments on DNA translocation through a nanopore [Kasianowicz *et al*., 1996; Meller *et al*., 2000], we first test the suitability and validity of our *multiscale* method to these kind of biophysical processes. Apart from the biological importance of these phenomena (in viral injection by phages, etc.), these are believed to open a way for ultrafast DNA-sequencing by reading the base sequence as the biopolymer passes through a nanopore. Experimentally, translocation is observed *in vitro* by pulling DNA molecules through micro-fabricated solid state or membrane channels under the effect of a localized electric field [Kasianowicz *et al*., 1996; Meller *et al*., 2000]. Here, a force is applied at the pore region that pulls the molecule through the pore in the presence of a fluid solvent. We performed a series of simulations for different initial realizations of the DNA structure and various lengths. A snapshot of such an event for a 6 kbp biopolymer is depicted in Figure 6.1.19(a). By accumulating all events for all lengths, duration histograms were constructed (see inset of Figure 6.1.19(b), where all the events for a 2.4 kbp long DNA have been projected into a histogram). The most probable time for each distribution defines the translocation time for the corresponding length. From this, a nonlinear relation between the translocation time ($\tau$) and the length (L) is

obtained ($\tau \sim L^{\alpha}$) and is shown in Figure 6.1.19(b). The exponent in this expression is $\tau \approx$ 1.28 ± 0.01, in a suprisingly good agreement with recent experimental observations [Storm *et al*., 2005]. This agreement motivates us to further explore the statistical and dynamical features of the translocation process. The scaling exponents can be justified on the basis of mean field representation of the biopolymer as a pair of compact blob configurations at either side of the pore, supplemented with observational data from the simulations. Finally, the work per time step performed on the biopolymer by the fluid and the pulling force were monitored and found almost constant throughout the process, apart from the end points. At these end points the polymer cannot be described by the blob picture and the related static scaling laws are violated.

## 2. Multiscale Model of Electronic Behavior in Stretched DNA

Within the context of *multiscale modeling* of biological systems, we have implemented a method to derive effective Hamiltonian models that are able to describe the dynamics of conduction and valence electrons in stretched DNA. The mechanism of charge transport in DNA has been the subject of numerous studies, with interest fuelled recently by both biological and technological considerations and it has been argued that it would be relevant for biology and biotechnology. In the case of stretched DNA, the applied external forces lead to distortions, imposed at the mesoscopic or macroscopic scales, which are bound to have a dramatic effect on electronic properties at the atomic scale and on electrical transport along DNA. Accordingly, a *multiscale* approach between different length scales is necessary to capture the electronic behavior of stretched DNA. To construct such a model, we begin with accurate density-functional-theory [Hohenberg and Kohn, 1964; Kohn and Sham, 1965; Perdew and Zunger, 1981] calculations for electronic states in DNA bases and base pairs in various relative configurations encountered in the equilibrium and stretched forms (Fig. 6.1.20(a)). These results are complemented by semi-empirical quantum mechanical calculations for the states of a small size dry DNA sequence. The calculated electronic states are then used to parameterize an effective tight-binding model that can describe electron hopping in the presence of environmental effects. We were able to show *quantitatively* that stretching of DNA dramatically narrows the width of the HOMO-LUMO gap. As a result, a small amount of disorder produced by environmental factors, will naturally lead to localization of the electrons along the DNA, as was observed in this work and in agreement with recent experiments [Heim *et al*., 2004]. This provides direct validation for the consistency of the *multiscale* method.
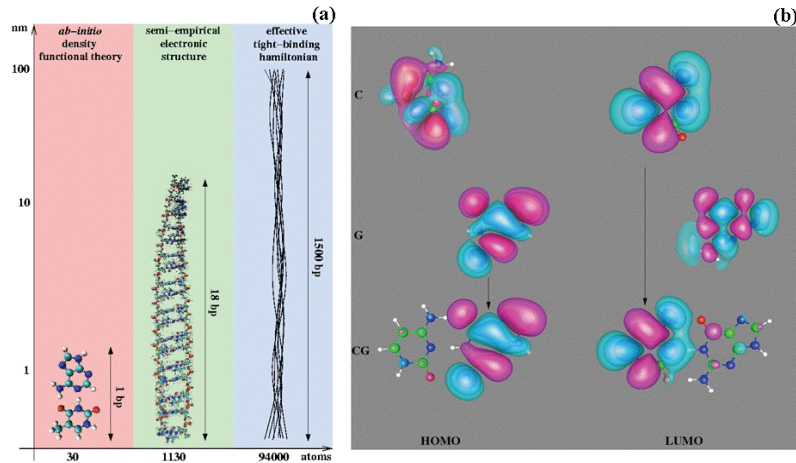
**Figure 6.1.20.** (**a**) Schematic illustration of the different scales included in our *multiscale* model: The two pictures on the left are atomistic systems simulated with the different computational approaches used here (*ab initio* density functional theory and semi-empirical electronic structure, respectively). The picture on the right represents a rope composed of DNA molecules, as in experiments [Heim *et al.*, 2004], which is treated by an effective tight-binding Hamiltonian constructed from the atomistic scale calculations. (**b**) Representative wave functions of frontier states (HOMO and LUMO) associated with the bases C and G and the base pair CG; these wave functions are not altered much in the DNA double helix, but the overlap between wave functions at adjacent base pairs, which controls transport along DNA, can be severely affected by the degree of stretching of the molecule.

# References

Heim, T. *et al.*, *Appl. Phys. Lett.* **85**, 2637 (2004).

Hohenberg, P. and W. Kohn, *Phys. Rev.* **136**, B864 (1964).

Kasianowicz, J.J. *et al.*, *Proc. Nat. Acad. Sci.*. USA **93**, 13770 (1996).

Kohn, W. and L.J. Sham, *Phys. Rev.* **140**, A1133 (1965).

A. Meller *et al.*, *Proc. Natl Acad. Sci.*. USA **93**, 1079 (2000).

Murphy, C.J. *et al.*, *Science* **262**, 1025 (1993).

Perdew, J.P. and A. Zunger, *Phys. Rev.* B **23**, 5048 (1981).

Storm, A.J. *et al.*, *Nanolett.* **5**, 1193 (2005).

S. Succi, *The Lattice Boltzmann Equation*, Oxford University Press, Oxford (2001).

Wolf-Gladrow, D.A., *Lattice Gas Cellular Automata and Lattice Boltzmann Models*, Springer Verlag, New York (2000).

# Immunomodulating Nano-Platforms for Combating Lung Infection

**Joseph P. Mizgerd**
Biology and Public Health, Harvard University
*Collaborator*: George M. Whitesides (Chemistry, Harvard)

Manipulating innate immune responses during infection will allow us to maximize antimicrobial efficacy while minimizing bystander tissue damage. Innate immune responses depend on polyvalent molecular interactions. We propose to develop tools for manipulating innate immunity in the lungs, in which molecules binding microbial surfaces or host cell receptors will function as immunomodulating agents when they are presented by nanomaterial scaffolds facilitating polyvalent interactions.

Polyvalency enhances avidity of adhesion, useful for targeting nanomaterials to cells, microbes, or tissues. Polyvalency cross-links receptors, sufficient to generate intracellular signaling cascades. For these reasons, otherwise inactive small molecules may become functional when presented on nanoscaffolds. Furthermore, platforms presenting multiple different small molecules can generate unique functionalities, eliciting distinct signaling cascades or cellular attachments. A variety of nanoscaffolding materials may be useful for such purposes, including polymers (e.g., of acrylamide) and solids (e.g., of gold), and the functionality of such nanoscaffolds may be determined in part by properties of the nanoscaffold including size, shape, and surface chemistry. Our long-term goal is to design and test new nanoscale tools for amplifying lung innate immune responses when and where they mediate antimicrobial host defense while dampening these responses when and where they cause inflammatory injury. We envision nanomaterials (i) mediating the ingestion and killing of bacteria by phagocytes, (ii) enhancing the recruitment and activation of phagocytes in the lung, and (iii) protecting lung cells from inflammatory damage.

We have demonstrated proof of principle for the first of these concepts, nanomaterials mediating phagocytosis (as reported in *Biomaterials* **27**, 3663–3674, 2006). We have examined these bivalent polymers in a variety of normal and immuno-suppressed mouse hosts, and during a variety of microbial infections of varied virulence characteristics. Although the polymers we have examined so far are capable of improving the ingestion of microbes by phagocytes in test tubes, this specific strategy has yet to prove effective when tested in living animals with virulent infections. Based on our results, we hypothesize that the capsule of virulent bacteria prevents phagocytes from recognizing nanoscale polymers adhered to the cell wall. This suggests an alternative strategy for attaching such bivalent polymers to the surfaces of bacteria, targeting the capsule rather than the cell wall of the bacteria. We are consulting with microbiologists to identify motifs that are conserved across capsules and potentially targeted by small molecules that can be attached to nanoscaffolds such as bifunctional polymers.

The second of these major concepts, the generation of nanomaterials designed to recruit and activate phagocytes in the lungs, is being actively pursued but is earlier in its development. The underlying idea is that weak binders to immune receptors can become

strong ligands which cross-link and signal through these receptors if they are presented in a polyvalent fashion by nanoscaffolds. If successful, such strategies may be effective at targeting a wide variety of immune receptors in the lungs and may be capable of improving host defenses against a wide variety of microbes causing lung infection. We have molecular targets in mind, and for two of these targets we were able to find evidence in the literature for small peptides purportedly binding them. **Whitesides**' group provided us with peptides (as free monomers) as well as with the same peptides attached to polymeric scaffolds. For one of these peptides, we have performed extensive studies sufficient to demonstrate that the free peptides behaved different than expected based on prior publications by another group. While positive controls demonstrated that our biological systems were well designed to detect the expected biological signals (in this case, activation of the transcription factor NF-$\kappa$B), neither the free peptides, nor the polymers, nor the polymers presenting polyvalent peptides proved efficacious at signaling, in either *in vitro* or *in vivo* settings. Because the peptides themselves did not produce the expected results, this lack of signaling does not argue against the eventual success of the strategy. Importantly, the lack of inflammatory signaling in living lungs treated with the polymer constructs bodes well for the safety of such agents when applied as potential therapeutics. In collaboration with members of **Whitesides**' group, we are pursuing other small molecules designed to interact with immune receptors in the lungs. Our strategy is first to identify small molecules that interact with the receptors of interest, second to determine whether polyvalent presentation of these ligands improves signaling from these receptors, and third to test the efficacy of these novel nanomaterials in improving host defenses during experimental pneumonias in mice.